

# The C-Terminal Domain of HU-Related Histone-like Protein Hlp from *Mycobacterium smegmatis* Mediates DNA End-Joining<sup>†</sup>

Anirban Mukherjee, Gargi Bhattacharyya,<sup>‡</sup> and Anne Grove\*

Department of Biological Sciences, Louisiana State University, Baton Rouge, Louisiana 70803

Received January 3, 2008; Revised Manuscript Received June 25, 2008

**ABSTRACT:** Histone-like proteins (such as HU, H-NS, and Fis) participate in nucleoid organization and in DNA replication, recombination, and transcription. Cold shock and anoxia upregulates a homologue of HU (Hlp) in *Mycobacterium smegmatis*, the nonpathogenic model of *Mycobacterium tuberculosis*. We show using electrophoretic mobility shift assays that Hlp, which in addition to the HU fold has a basic C-terminal tail containing multiple PAKK and PAAK repeats, has very high affinity for DNA. The affinity of Hlp for 76 bp linear DNA is higher,  $K_d = 0.037 \pm 0.001$  nM, compared to an Hlp variant without the C-terminal repeats,  $K_d = 2.5 \pm 0.1$  nM and the isolated C-terminal repeat domain,  $K_d = 0.8 \pm 0.2$  nM, where  $K_d$  in all cases reflects an aggregate affinity for the DNA probes, not the affinity for binding to a single site. Hlp lacking the entire C-terminal domain binds DNA only poorly. These data indicate that both Hlp domains contribute to high-affinity DNA binding. Hlp promotes DNA end-joining in the presence of T4 DNA ligase, and this property is mediated by the C-terminal repeats. At <100 nM concentration, Hlp represses transcription by T7 RNA polymerase *in vitro* whereas the individual N- and C-terminal domains do not, even when present together. Notably, while DNA end-joining can be achieved by the isolated C-terminal domain, transcriptional repression requires for both domains to be present on a single polypeptide. Given the low cellular concentration of Hlp, our data suggest that its primary functional role may be in DNA-dependent responses to environmental stress rather than in nucleoid organization.

The bacterial nucleoid contains numerous small basic proteins known as histone-like proteins that are involved in the organization of genomic DNA as well as in DNA replication, recombination, repair, and transcription (1–4). Of these histone-like proteins, *Escherichia coli* HU, the most extensively studied HU, exists primarily as a heterodimer of two homologous ~9 kDa subunits, though the presence of higher oligomeric forms has also been proposed (3). Most other HU proteins are homodimeric. HU dimers form an  $\alpha$ -helical body from which two  $\beta$ -arms protrude and mediate DNA binding (6–9). Binding of HU dimers to DNA, as seen for example from the *Anabaena* HU-DNA cocrystal structure, involves intercalation of proline residues from both  $\beta$ -arms between DNA base pairs resulting in DNA bend angles of 105–139° (9). Most HU proteins bind double-stranded DNA non-sequence specifically and with low affinity, and several, such as *E. coli* HU, have markedly higher affinity for DNA containing nicks, gaps, single-strand breaks, and four-way junctions (10–16).

HU proteins play a significant role in modifying nucleoid architecture, and they are involved in many intracellular processes, mainly through mediating changes in DNA topology. For example, *E. coli* HU forms a multiprotein–DNA complex in association with GalR and represses transcription

at the *gal* promoter (17). It also promotes the DnaA-dependent opening of replication origin *oriC* in *E. coli* by stabilizing the open complex (7, 9, 18). HU proteins generally restrain negative supercoiling in the presence of topoisomerase I (14, 16, 19). *Bacillus subtilis* HU (HBsu)<sup>1</sup> and *E. coli* HU stabilize recombination intermediates (10, 20), and HU from the hyperthermophilic eubacterium *Thermotoga maritima* and from *B. subtilis* have been shown to be involved in DNA compaction *in vivo* (21, 22).

Mycobacterial histone-like proteins (Hlp) are different from other eubacterial HU proteins, and not much is known about their DNA binding properties or intracellular functions. Hlps are larger compared to other HU proteins and have an additional C-terminal domain, largely composed of proline, alanine, and lysine residues assembled in numerous repeats that resemble the (S/T)PKK repeats of eukaryotic histone H1 proteins. The N-terminal domain of Hlp bears significant sequence homology to HU proteins. Consistent with conservation of the HU fold, Hlp from *Mycobacterium tuberculosis* has been shown to interact with DNA (23). The 27 kDa Hlp from *Mycobacterium smegmatis* is upregulated under cold shock-induced dormancy and anoxia, and *hlp* deletion strains of *M. smegmatis* are unable to recover metabolically from cold shock-induced dormancy, indicating a possible involvement of Hlp in DNA metabolism (24, 25).

<sup>†</sup> Supported by the National Science Foundation (MCB-0414875 and MCB-0744240 to A.G.).

\* Corresponding author. Tel: 225-578-5148. Fax: 225-578-8790. E-mail: agrove@lsu.edu.

<sup>‡</sup> Present address: East India Pharmaceutical Works Ltd., Kolkata, India.

<sup>1</sup> Abbreviations: Hlp, histone-like protein; RT-Hlp, repeatless histone-like protein; CTR, C-terminal repeats; EMSA, electrophoretic mobility shift assay; TmHU, *Thermotoga maritima* HU; HBsu, *Bacillus subtilis* HU; DrHU, *Deinococcus radiodurans* HU; HpyHU, *Helicobacter pylori* HU; NHEJ, nonhomologous end-joining; IHF, integration host factor.

*M. smegmatis* Hlp has been suggested to be a membrane-associated laminin-binding protein despite lacking a membrane localization signal sequence (26). However, using antihistone H1 antibody we have seen Hlp to colocalize with the *M. smegmatis* nucleoid (unpublished observation). Notably, Hlp is not as abundant as other HU proteins *in vivo*; only approximately 1000 molecules are present per cell after upregulation (unpublished observation) as compared to ~30000 HU molecules in *E. coli* (3). Here we show that *M. smegmatis* Hlp has two DNA binding domains, both of which participate in high-affinity DNA binding. A unique feature of Hlp is its ability to enhance DNA end-joining *in vitro*.

## MATERIALS AND METHODS

**Cloning, Mutagenesis, and Protein Purification.** The *hlp* gene was amplified from *M. smegmatis* genomic DNA (forward primer 5'-ATGAACAAAGCGGAGCTCATC-GACG-3' and reverse primer 5'-TTTACCTGCGGCCCT-TCTTGGCC-3') and cloned into pCR T7/NT-TOPO plasmid (Invitrogen) generating pHlp, expressed with an N-terminal His<sub>6</sub> tag followed by an enterokinase cleavage site. The integrity of the construct was confirmed by sequencing. For overexpression, pHlp was transformed into *E. coli* BL21(DE3)-pLysS. The cells were grown from a single colony at 37 °C, 250 rpm, in LB with ampicillin (100 µg/mL) until OD<sub>600</sub> ~ 0.2 and then induced for 1 h by adding isopropyl β-D-thiogalactopyranoside (IPTG) to a final concentration of 1 mM. Recombinant Hlp is expressed abundantly in *E. coli* (provided induction during early exponential phase). The cells were harvested and stored at -80 °C.

All steps during Hlp purification were conducted at 0–4 °C. Pellets were thawed on ice and resuspended in 50 mL of cell lysis buffer (50 mM Tris-HCl (pH 8.0), 0.25 M NaCl, 5 mM Na<sub>2</sub>EDTA, 5% (v/v) glycerol, 5 mM 2-mercaptoethanol, 0.1 mM phenylmethanesulfonyl fluoride (PMSF)). Lysozyme was added to a final concentration of 200 µg/mL and 10% Triton X 100 to 0.05% final concentration, and the mixture was incubated on ice for 1 h. Thirteen percent polymin P (BASF) was added dropwise to a final concentration of 0.5%. The cell lysate was centrifuged at 9K rpm (GSA rotor) at 4 °C for 20 min. The supernatant was collected and dialyzed against phosphate buffer (15 mM K<sub>2</sub>HPO<sub>4</sub>, 9 mM KH<sub>2</sub>PO<sub>4</sub>, 0.12 M KCl, 4.8% glycerol (v/v), 5 mM 2-mercaptoethanol, 0.1 mM PMSF) overnight at 4 °C. Cobalt beads (TALON metal affinity resins; BD Biosciences) were resuspended as per manufacturer's protocol, and 1 mL of the resin was washed three times with 10 bed volumes of phosphate buffer. The dialyzed cell lysate was incubated with the metal affinity beads for 1 h at 4 °C on a rocker and was loaded onto a gravity flow column. After three washes, proteins were eluted with 150 mM imidazole-containing phosphate buffer. The purest fractions, identified from Coomassie blue stained SDS–polyacrylamide gels, were pooled and dialyzed against low salt Tris buffer (20 mM Tris-HCl (pH 8.0), 50 mM KCl, 5% (v/v) glycerol, 1 mM Na<sub>2</sub>EDTA, 3.5 mM 2-mercaptoethanol, 0.2 mM PMSF) and loaded on a CM-Sephadex column equilibrated with the same buffer. The protein was eluted with a linear gradient of 50 mM to 1 M KCl. The purest fractions were again pooled and dialyzed against the phosphate buffer and subjected to batch mode purification on cobalt beads as described above.

Purity of the protein was assessed by Coomassie blue and silver staining of SDS–PAGE gels. Protein concentration was determined by densitometric analysis of Coomassie-stained SDS–PAGE gels using BSA standards, as Hlp contains no Trp or Tyr that would allow spectrophotometric quantitation. However, we have found no reason to suspect that HU homologues exhibit unusual dye-binding properties, as evidenced by side-by-side comparison of dye binding by BSA and the HU homologue TF1 (which does contain a single tyrosine; hence its concentration may be determined spectroscopically). Lower molecular mass fragments likely represent in part truncated transcripts.

Mutant proteins were created by whole plasmid PCR-based mutagenesis of the *Hlp* gene, creating pRL-Hlp by inserting a stop codon at the 119th residue and creating pTL-Hlp by introducing a stop codon after the 97th residue. pCTR was created by amplification of the C-terminal repeat region followed by cloning into pCR T7/NT TOPO (Invitrogen). Integrity of the constructs was established by sequencing. Primers used to create pRL-Hlp were 5'-CCAAGAAGGC-CTAAAAGAAGGCACC-3' and 5'-CGGGACCAGCCGT-GAC-3'. Primers used to create pTL-Hlp were 5'-GCACA-GAAGTAACCGGCCGATG-3' and 5'-GCCAGAGATAA-CCGCCTTGAAC-3', and primers used to amplify the CTR region were 5'-AAGCGTGGCATATGCGCTGGTCC-3' and 5'-GGATCAAGCCTCGAATTCCGGGAA-3'. Expression constructs were transformed into *E. coli* BL21(DE3)pLysS; cells were grown in LB media at 37 °C, 250 rpm, until OD ~ 0.2 and induced with 1 mM IPTG for 1 h; cells were harvested by centrifugation and stored at -80 °C. Proteins were purified as described for full-length Hlp and stored in aliquots at -20 °C. HU homologues from *Thermotoga maritima* (TmHU), *B. subtilis* (HBSu), *Helicobacter pylori* (HpyHU), and *Deinococcus radiodurans* (DrHU) were purified as previously described (13–16).

**Electrophoretic Mobility Shift Assays (EMSA) and Calculation of Binding Constants.** Seventy-six nt oligonucleotides used for EMSA were purchased and purified by denaturing gel electrophoresis. The top strand (5'-CGC TGC AAT CTC TTT TTC AAT TGC TCC GGA CTG TAA ATT GGC GGT CCC TTA CTC TTT CCT CAA CAA TTA ACG GCC C-3') was <sup>32</sup>P-labeled at the 5'-end with T4 polynucleotide kinase, and complementary strands were annealed as described (15). The four-way junction was created as previously described and <sup>32</sup>P-labeled at the 5'-ends with T4 polynucleotide kinase (15). DNA and protein were incubated in 1× binding buffer (20 mM Tris-HCl (pH 8.0), 10 mM MgCl<sub>2</sub>, 50 mM NaCl, 0.1 mM Na<sub>2</sub>EDTA, 0.1 mM DTT, 0.05% (w/v) Brij58) in a 10 µL reaction volume for 20 min at room temperature. Five femtomole labeled DNA was titrated with increasing concentrations of proteins. Complexes were electrophoresed on 5% (w/v) polyacrylamide gels (39:1 acrylamide:bisacrylamide) in TBE (45 mM Tris–borate (pH 8.3), 1 mM EDTA). Gels were prerun for 30 min at 175 V at room temperature and then for 1.5 h after loading the samples. Gels were dried, and protein–DNA complexes were visualized by phosphorimaging using ImageQuant 1.1. For densitometric quantitation, regions above the free DNA were considered as complex. Relative complex formation was plotted as a function of protein concentrations and fitted to the Hill equation,  $f = f_{\max}[\text{Hlp}]^n / K_d(1 + [\text{Hlp}]^n / K_d)$ , where  $f$  is fractional saturation,  $f_{\max}$  is 100% complex

formation, [Hlp] is concentration of proteins,  $n$  is Hill coefficient, and  $K_d$  reflects binding to the entire DNA construct; note that the  $K_d$  does not report on the affinity for a single site but merely allows a semiquantitative comparison of the aggregate affinity for the DNA probe for the different protein variants. For calculation purposes, the initial value of  $f_{\max}$  was 100 and for  $n$  and  $K_d$ , 1. All experiments were performed at least three times.

**Competition Assay.** Plasmid pUC18 was linearized by *Eco*RI digestion followed by phenol extraction and ethanol precipitation. Five femtomoles of Hlp was incubated with  $^{32}$ P-labeled 76 bp DNA in  $1\times$  binding buffer in a total 10  $\mu$ L reaction volume at room temperature for 15–20 min. Linearized pUC18 was added in increasing amounts as a cold competitor, and the reactions were incubated another 15–20 min at room temperature. Reactions were subjected to electrophoresis as described above. All reactions were carried out at least in duplicate.

**End-Joining Assays.** DNA substrates, 105 bp and 315 bp DNA, were created by digestion of pET5a by BspHI followed by gel purification and  $^{32}$ P-labeling of the 5'-ends with T4 polynucleotide kinase. Five femtomoles of labeled 105 or 315 bp DNA was incubated in each reaction with increasing amounts of Hlp, RL-Hlp, or CTR in a total 10  $\mu$ L reaction volume containing  $1\times$  binding buffer and  $1\times$  NEB ligase buffer for 15–0 min at room temperature followed by 1 h room temperature incubation with 40 units of T4 DNA ligase (New England Biolabs). For positive control reactions, *T. maritima* HU was used, and reactions were treated with 100 units of exonuclease III for 30–45 min at room temperature to distinguish circular and oligomeric species. Reactions were then subjected to phenol extraction and ethanol precipitation followed by resuspension in 10  $\mu$ L of TE and subjected to gel electrophoresis as described above.

For comparison of DNA end-joining by other HU proteins, 5 fmol of 5'-end  $^{32}$ P-labeled 105 bp DNA was incubated with similar concentrations of *T. maritima* HU, Hlp, *B. subtilis* HU, *H. pylori* HU, and *D. radiodurans* HU with  $1\times$  binding buffer and  $1\times$  NEB ligase buffer for 15–20 min at room temperature followed by incubation with T4 DNA ligase at room temperature for 1 h. The reactions were treated as described above. All reactions were carried out at least in duplicate.

**In Vitro Transcription Assay.** One microgram of supercoiled pTL-Hlp was used as template for *in vitro* transcription assays in a total 30  $\mu$ L reaction volume.  $\alpha$ - $^{32}$ P-UTP ( $10^7$  cpm) and 20  $\mu$ M GTP, 10  $\mu$ M ATP and CTP, and 2.5  $\mu$ M UTP were used per reaction with  $1\times$  T7 RNA polymerase buffer. DNA template and polymerase buffer were mixed first, and 1  $\mu$ L of T7 RNA polymerase (New England Biolabs) and increasing amounts of Hlp, RL-Hlp, CTR of Hlp, or equimolar mixtures of RL-Hlp and CTR were added in each reaction followed by 20 min room temperature incubation. The rNTP mix was added to start each reaction and incubated for another 20 min at room temperature. Reactions were stopped by adding 70  $\mu$ L of stop solution (5 M  $\text{NH}_4\text{OAc}$ , 0.014 ng/ $\mu$ L tRNA,  $^{32}$ P-labeled 76 nt recovery marker) followed by phenol extraction and ethanol precipitation and resuspension of the transcripts in 20  $\mu$ L of formamide loading buffer. Samples were loaded on a 5% (w/v) denaturing polyacrylamide gel. Gels were prerun for 30 min at 600 V

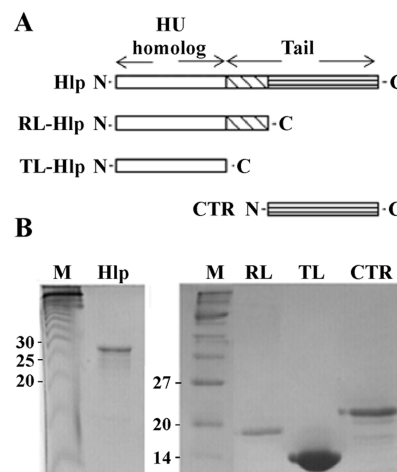


FIGURE 1: Histone-like protein (Hlp) from *M. smegmatis*, different domains, and mutant proteins. (A) Schematic representation of the N-terminal bacterial HU homologous domain (open box) and the C-terminal tail. Mutant protein lacking the entire C-terminal tail is tail-less Hlp (residues 1–97, TL-Hlp). Protein representing the C-terminal tail has proline-, alanine-, and lysine-rich repeats and is termed CTR (C-terminal repeats). Mutant protein lacking only the repeat region is repeat-less Hlp (residues 1–118, RL-Hlp). (B) Purified Hlp and mutant proteins. Different protein levels reflect gel loading, not relative levels of expression. Molecular mass markers are indicated in kDa.

before loading the samples and then for 1 h. Gels were dried, and transcripts were visualized by phosphorimaging. Reactions were carried out at least in triplicate.

**Preparation of Total RNA from *M. smegmatis*.** Total RNA was purified from exponentially growing *M. smegmatis* ( $\text{OD}_{600} = 0.1$ ), from cells exposed to 24 h of cold shock at 10  $^{\circ}\text{C}$ , and from cells grown for 1 h at 37  $^{\circ}\text{C}$  after cold shock using RNeasy Mini Kit (Qiagen) with modification of the protocol supplied by the manufacturer. Cells were incubated with lysozyme at 37  $^{\circ}\text{C}$  for 1 h to achieve complete cell lysis. Total RNA was loaded on 1% agarose gel and visualized by ethidium bromide staining. One microgram of ssRNA ladder was used (New England Biolabs). Reactions were carried out at least in duplicate.

## RESULTS

**High-Affinity DNA Binding by *M. smegmatis* Hlp Involves Two DNA Binding Domains.** *M. smegmatis* Hlp contains 212 amino acids whereas most HU homologues are composed of  $\sim 90$  amino acids. The N-terminal Hlp domain is homologous to HU proteins and is predicted to adopt the characteristic fold. Of the remaining residues, a series of proline-, alanine-, and lysine-rich repeats constitute the C-terminal repeat region (CTR) (Figure 1A). To determine the role of each domain in DNA binding, a mutant protein was created that represents the 97-residue N-terminal HU-homologous domain, referred to as tail-less Hlp (TL-Hlp) (Figure 1B). The truncation after residue 97 to generate TL-Hlp was selected as it corresponds to the average length of HU homologues IHF and TF1 (as compared to the 90-residue length common for HU homologues). Another truncated protein was created that represents the N-terminal domain including the part of the C-terminal extension not featuring the proline-, alanine-, and lysine-rich repeats, named repeat-less-Hlp (RL-Hlp), as well as a mutant protein representing



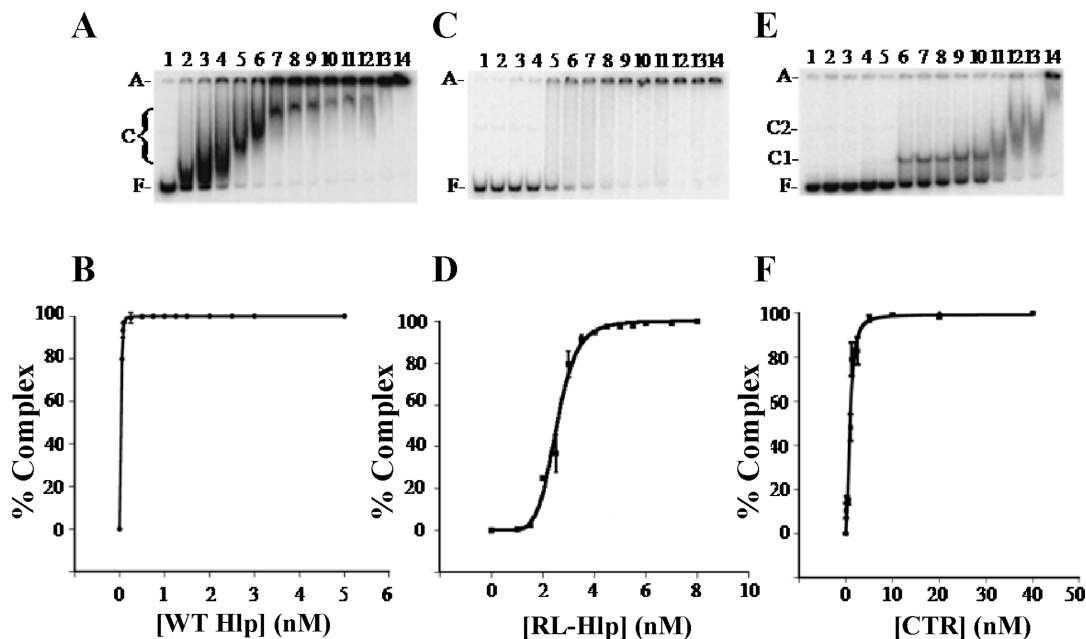


FIGURE 2: Binding of Hlp and mutant proteins to 76 bp DNA. (A) Hlp binding (0, 0.05, 0.075, 0.1, 0.25, 0.5, 0.75, 1, 1.25, 1.5, 2, 2.5, 3, and 5 nM, respectively, in lanes 1–14), (C) RL-Hlp binding (0, 0.1, 0.25, 0.5, 1, 1.25, 1.5, 1.75, 2, 2.5, 5, 10, 20, and 40 nM, respectively, in lanes 1–14), and (E) CTR binding (0, 1, 1.5, 2, 2.5, 3, 3.5, 4, 4.5, 5, 5.5, 6, 7, and 8 nM, respectively, in lanes 1–14) to 76 bp DNA. (B), (D), and (F) represent the corresponding binding isotherms. Error bars represent standard deviation of the mean. Free DNA (F), complex (C), and aggregates (A) are identified at the left.

only the CTR (Figure 1B). During overexpression, T7 RNA polymerase is prone to producing incomplete transcripts while transcribing through  $d(C)_n \cdot d(G)_n$  sequence (27); the faster migrating species seen in SDS–PAGE gels are therefore likely in part produced due to incomplete transcription by T7 RNA polymerase of the numerous  $d(C)_n \cdot d(G)_n$  repeats of the gene sequence encoding the C-terminal domain, in turn producing the truncated protein fragments seen with Hlp and CTR. For full-length Hlp and CTR, these truncated His-tagged species likely bind DNA, but with lower affinity than the corresponding full-length protein (see below). Combined with their lower concentration, the effect on DNA binding assays is likely to be limited.

As expected from its homology to other bacterial HU proteins, *M. smegmatis* Hlp binds DNA but with unusually high affinity. A 76 bp duplex with average G+C content was chosen that does not have propensity for adopting noncanonical structure as evidenced by uniform cleavage with methidiumpropyl-EDTA-Fe(II) (28). As seen from electrophoretic mobility shift assays (EMSA), Hlp binding to 76 bp DNA leads to complexes of reduced mobility and at higher concentrations to aggregates that are unable to enter the gel matrix (Figure 2A.) When the percent complex formation is plotted as a function of protein concentration and the data are fitted to the Hill equation, a  $K_d$  of  $0.037 \pm 0.001$  nM (Figure 2B) is obtained, which indicates that Hlp has much higher affinity for double-stranded DNA compared to other bacterial HU homologues (note, however, that the  $K_d$  obtained from fits of the data to the Hill equation does not reflect the affinity for a single site). While the data are fitted well to a hyperbolic binding isotherm, Hlp saturates the DNA at a very low concentration with only few data points below the apparent  $K_d$ , and cooperative binding therefore cannot be ruled out. The N-terminal His<sub>6</sub> tag does not appear to affect interaction with DNA, as evidenced by equivalent levels of complex formation with plasmid DNA

for His<sub>6</sub>-tagged Hlp and enterokinase-cleaved Hlp lacking the His<sub>6</sub> tag (data not shown).

The repeat-less Hlp (RL-Hlp) binds to 76 bp DNA and forms complexes seen as smears and as aggregates unable to enter the gel matrix (Figure 2C). The  $K_d$  determined from fits of the data to the Hill equation is  $2.5 \pm 0.1$  nM (Figure 2D), significantly higher than the full-length protein, indicating a lower affinity; the Hill coefficient of  $n = 6.5$  reflects significant positive cooperativity. The C-terminal repeat region also binds DNA with high affinity (Figure 2E), and it forms complexes of defined mobility as well as smears and aggregates at higher concentrations. The binding constant for this interaction is  $0.8 \pm 0.2$  nM (Figure 2F), intermediate between that of Hlp and RL-Hlp. Evidently, the N-terminal HU-homologous region and the C-terminal domain resembling eukaryotic histone H1 domain can independently bind double-stranded DNA with high affinity.

A discrete band representing a protein–DNA complex would be expected for site-specific binding or for the formation of a predominant complex of defined stoichiometry and topology that is stable to electrophoresis. That Hlp, in contrast to CTR, does not form complexes with defined mobility suggests that either the topology of the DNA in complex with Hlp is variable leading to different electrophoretic mobility, perhaps as a function of the position of the protein relative to DNA ends, that Hlp does not form complexes with a preferred stoichiometry, and/or that complexes dissociate during electrophoresis. While the full-length Hlp and CTR appear to bind to 76 bp DNA noncooperatively (Figure 2B,F), RL-Hlp binding is cooperative (Figure 2D), perhaps suggesting that removal of the CTR exposes protein–interaction surfaces.

Competition assays were performed with supercoiled and linear plasmid DNA as cold competitors to <sup>32</sup>P-labeled 76 bp DNA as substrate for Hlp, which revealed that Hlp has no binding preference for either supercoiled or linear DNA

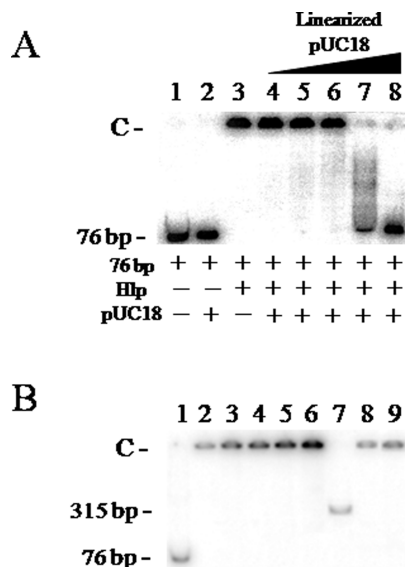


FIGURE 3: Nonsequence specific binding and substoichiometric saturation of DNA by Hlp. (A) Linearized plasmid DNA competes for Hlp-complex formation with 76 bp DNA. All reactions contain 10 fmol of 76 bp DNA (760 fmol of base pairs). Lane 1, 76 bp DNA only; lane 2, 76 bp DNA and pUC18. Lanes 3–8 contain 5 nM Hlp and 0, 270, 540, 760, 1075, and 1350 fmol of base pair of plasmid pUC18, respectively. (B) Titration of Hlp with increasing concentration of labeled 76 or 315 bp DNA. Lane 1, 76 bp DNA (50 fmol); lane 7, 315 bp DNA (20 fmol). Reactions in lanes 2–6 contain 50, 100, 150, 200, and 250 fmol of 76 bp DNA, respectively, and 50 fmol of Hlp. Reactions in lanes 8 and 9 contain 50 and 100 fmol of 315 bp DNA, respectively, and 50 fmol of Hlp. Complexes are identified as C.

(data not shown). When preformed complexes with 76 bp DNA containing the equivalent of 760 nM base pair were challenged with linear pUC18, the complexes dissociated; as seen in Figure 3A, lanes 5 and 6, addition of 540 and 760 nM base pair of competitor DNA causes the existing complex of 76 bp DNA and Hlp to dissociate. Approximately 1075 nM base pairs of cold competitor cause complete loss of 76 bp Hlp complex (Figure 3A, lane 7). That Hlp is competed off the 76 bp DNA by an equivalent molar concentration of pUC18 base pairs indicates that it binds DNA without sequence specificity. Consistent with the presence of two DNA binding domains, Hlp saturates DNA under substoichiometric conditions (Figure 3B). Fifty femtomoles of Hlp can saturate 250 fmol of 76 bp DNA (Figure 3B, lane 6) and 100 fmol of 315 bp DNA (lane 9), indicating that both domains can interact with DNA independently. We do not ascribe a physical meaning to the binding ratio, which is likely to be variable depending on the length of the DNA duplex due to steric effects. It has been previously shown that the divalent nature of eukaryotic histone H1 results in complexes with DNA that do not enter the gel matrix (29), likely due to formation of a network of interactions. We surmise, therefore, that Hlp forms similar networked complexes.

In contrast, the tail-less Hlp (TL-Hlp) representing the eubacterial HU-homologous region binds DNA only poorly (Figure 4). TL-Hlp forms complexes with DNA at very high concentrations, but complexes are unstable and dissociate during electrophoresis (Figure 4, lanes 7 and 8). The reduced affinity of TL-Hlp for DNA is possibly due to partial loss of domain structure responsible for DNA binding. Similar observations were made with integration host factor from

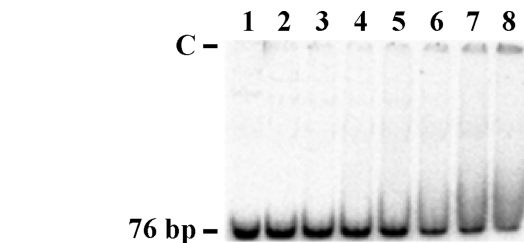


FIGURE 4: Binding of tail-less Hlp to 76 bp DNA. Lane 1, no protein; lanes 2–8, 0.05, 0.1, 0.25, 0.5, 1.2, 2.4, and 6.0  $\mu$ M TL-Hlp, respectively. All reactions contain 5 fmol of 76 bp DNA. Free DNA and complexes (C) are identified.

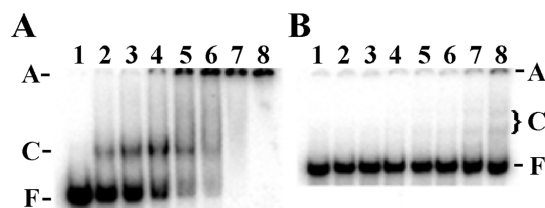


FIGURE 5: Hlp and RL-Hlp binding to four-way junction. (A) Hlp binding to four-way junction: lane 1, no protein; lane 2, 0.1 nM Hlp; lane 3, 0.25 nM Hlp; lane 4, 0.5 nM Hlp; lane 5, 0.75 nM Hlp; lane 6, 1 nM Hlp; lane 7, 2.5 nM Hlp; lane 8, 5 nM Hlp. (B) RL-Hlp binding to four-way junction with same protein concentrations as Hlp. Free DNA (F), complex (C), and aggregates (A) are identified at the left.

*E. coli* and TF1 (both type II DNA binding proteins), indicating the necessity of C-terminal amino acids succeeding the HU homologous domain in DNA binding (30–34).

Preferred binding to four-way junction DNA has been reported for several HU homologues (10, 15, 16). Hlp also binds to four-way junction DNA and forms complexes of defined mobility and eventually aggregates at concentrations similar to those required to saturate duplex DNA (Figure 5A.) The presence of a complex of defined mobility suggests that Hlp forms a specific complex with this DNA construct, albeit with a half-maximal saturation similar to that seen for the 76 bp DNA (which contains an equivalent total number of nucleotides). Removal of the C-terminal domain similarly reduces the affinity for four-way junction DNA (Figure 5B).

**Enhanced DNA End-Joining Is Mediated by the C-Terminal Domain.** The architectural roles of bacterial HU proteins depend on their ability to bend DNA. To assess DNA bending, DNA shorter than the persistence length was ligated by T4 DNA ligase; only in the presence of a DNA bending protein would intramolecular cyclization be seen, detectable as a product that is resistant to exonuclease-mediated degradation. As determined by this assay, *M. smegmatis* Hlp is not capable of cyclizing DNA, even under conditions of low DNA concentration that would favor intramolecular ring closure; instead, it enhances end-joining of DNA in the presence of T4 DNA ligase, forming dimer, trimer, and higher order oligomers (Figure 6.) In contrast, *T. maritima* HU (TmHU) bends 105 bp DNA to form monomer circles in the presence of T4 DNA ligase (Figure 6, lanes 6 and 7, and ref 22).

To address whether the ability to enhance DNA end-joining is unique to Hlp as compared to other HU proteins, a comparative analysis including Hlp, TmHU, *B. subtilis* HU (HBSu), *Helicobacter pylori* HU (HpyHU), and *Deinococcus radiodurans* HU (DrHU) was performed (Figure 7.) TmHU, HBSu, and HpyHU bend DNA and form monomer circles

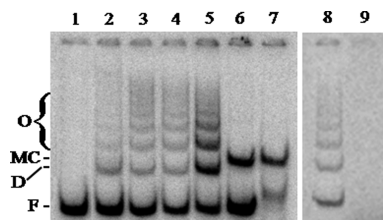


FIGURE 6: Hlp promotes DNA end-joining. Five femtomoles of 105 bp DNA was used per reaction in the presence of T4 DNA ligase. Lane 1, DNA only; lane 2, 1 nM Hlp; lane 3, 2.5 nM Hlp; lane 4, 10 nM Hlp; lane 5, 40 nM Hlp; lane 6, 0.1  $\mu$ M *T. maritima* HU; lane 7, 0.1  $\mu$ M *T. maritima* HU and exonuclease III. O, oligomers; MC, monomer circles; D, linear dimer; F, free DNA. Linear products (lane 8) were identified by their sensitivity to exonuclease III digestion (lane 9).

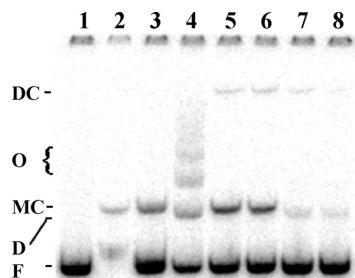


FIGURE 7: Among histone-like proteins only Hlp promotes DNA end-joining. DNA cyclization with 105 bp DNA and T4 DNA ligase. Lane 1, DNA only (100 fmol); lane 2, DNA cyclization in the presence of TmHU followed by treatment with DNA exonuclease III to show the cyclized species; lane 3, 100 nM TmHU; lane 4, 100 nM Hlp; lane 5, 100 nM *B. subtilis* HU; lane 6, 100 nM *H. pylori* HU; lane 7, 100 nM *D. radiodurans* HU; lane 8, only T4 DNA ligase. DC, dimer circle; O, oligomers; MC, monomer circles; D, linear dimers; F, free DNA.

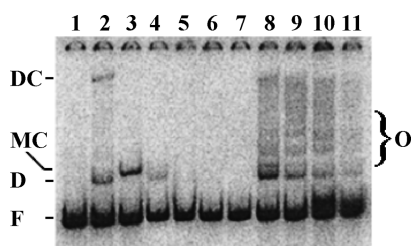


FIGURE 8: C-Terminal repeats (CTR) of Hlp mediate DNA end-joining. Five femtomoles of 105 bp DNA was used per reaction in the presence of T4 DNA ligase. Lane 1, DNA only; lane 2, T4 DNA ligase and DNA; lane 3, 0.1  $\mu$ M *T. maritima* HU; lane 4, 50 nM RL-Hlp; lane 5, 100 nM RL-Hlp; lane 6, 250 nM RL-Hlp; lane 7, 400 nM RL-Hlp; lane 8, 10 nM CTR; lane 9, 25 nM CTR; lane 10, 40 nM CTR; lane 11, 100 nM CTR. DC, dimer circle; O, oligomers; MC, monomer circles; D, linear dimers; F, free DNA.

in the presence of T4 DNA ligase (Figure 5, lanes 3, 5, and 6) but do not enhance end-joining under these conditions. DrHU and Hlp are both incapable of bending short DNA, and only Hlp is able to bring two DNA ends together (Figure 7, lane 4). This observation is consistent with high-affinity DNA binding by the individual N- and C-terminal Hlp domains.

The ability of Hlp to join DNA fragments can be attributed to the CTR. Unlike most other HU proteins, the N-terminal HU homologous domain of Hlp (RL-Hlp) does not cyclize 105 bp DNA (Figure 8, lanes 4–7) and also is not capable of enhancing end-joining. TL-Hlp, which binds DNA only poorly, also did not promote either DNA end-joining or DNA

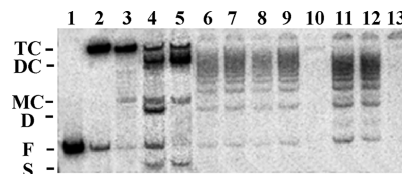


FIGURE 9: Hlp and CTR prevent DNA bending. Lane 1, free DNA (315 bp); lane 2, T4 ligase only; lane 3, T4 ligase and exonuclease III; lane 4, TmHU and T4 ligase; lane 5, TmHU, T4 ligase, and exonuclease III; lanes 6–9, 0.4, 0.5, 0.75, and 1  $\mu$ M CTR, respectively, with T4 ligase; lane 10, 1  $\mu$ M CTR, T4 ligase and exonuclease III; lanes 11 and 12, 0.2 and 0.3  $\mu$ M Hlp, respectively, with T4 ligase; lane 13, 0.3  $\mu$ M Hlp, T4 ligase, and exonuclease III. Trimer circle (TC), dimer circle (DC), monomer circle (MC), linear dimer (D), free DNA (F), and supercoiled DNA (S) are identified at the left.

cyclization (up to 6  $\mu$ M concentration; data not shown). In contrast, the isolated CTR facilitates joining of DNA ends, aiding in the formation of dimer, trimer, and other higher order oligomers (Figure 8, lanes 8–11). At the highest concentration, CTR appears to inhibit the reaction (lane 11), perhaps because the DNA becomes occluded and hence inaccessible to the DNA ligase. Under similar conditions, Hlp and CTR prevent DNA bending (Figure 9.) In the presence of T4 DNA ligase, 315 bp DNA, which is longer than the persistence length, primarily forms a trimer circle that is resistant to exonuclease digestion (Figure 9, lanes 2 and 3), and in the presence of TmHU and T4 ligase, monomer, dimer, and trimer circles are seen (Figure 9, lanes 4 and 5). When CTR and Hlp are present in the reactions, however, no circular species are generated; instead, end-joining products are formed (Figure 9, lanes 6–9 and 11–12); these products are effectively degraded by exonuclease III (Figure 9, lanes 10 and 13).

*M. smegmatis* Hlp Represses Transcription in Vitro. *E. coli* HU was previously reported to stimulate transcription by T7 RNA polymerase, prompting us to evaluate whether Hlp reproduces this effect (35). In contrast to *E. coli* HU, however, *M. smegmatis* Hlp represses T7 RNA polymerase, as evidenced by its ability to repress transcription of the TL-Hlp gene *in vitro* (Figure 10A.) When supercoiled pTL-Hlp was used as a template for transcription with T7 RNA polymerase, 0.083  $\mu$ M Hlp reduces transcript yield and 0.166  $\mu$ M and higher concentrations completely abolish transcription (Figure 10A, lanes 3–5). Under similar conditions, RL-Hlp and CTR are not capable of repressing transcription, though they retain a high affinity (nanomolar) for DNA (Figure 10A, lanes 6–8 and lanes 9–11). It is also significant that nonspecific association of the “poly-lysine”-like CTR with DNA is insufficient to cause transcriptional repression. Notably, equimolar concentrations of RL-Hlp and CTR together do not repress transcription (Figure 10A, lanes 12 and 13), and 0.33  $\mu$ M RL-Hlp and CTR together reduce the yield of transcripts only slightly (Figure 10A, lane 14), indicating that the individual domains cannot restore the full functionality of the full-length protein; for Hlp to act as a transcriptional repressor *in vitro*, both domains must be present on a single polypeptide. When linearized pTL-Hlp was used as a template for transcription, the patterns of transcriptional repression remain equivalent (data not shown), indicating that transcriptional repression is not a function of altered complex formation due to topological differences of the templates.



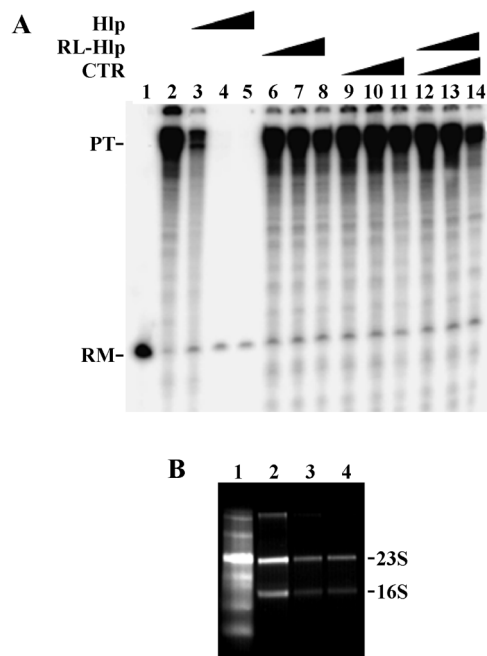


FIGURE 10: Hlp represses transcription. (A) lane 1, recovery marker only; lane 2, only T7 RNA polymerase; lane 3, 0.083  $\mu$ M Hlp; lane 4, 0.166  $\mu$ M Hlp; lane 5, 0.33  $\mu$ M Hlp; lane 6, 0.083  $\mu$ M RL-Hlp; lane 7, 0.166  $\mu$ M RL-Hlp; lane 8, 0.33  $\mu$ M RL-Hlp; lane 9, 0.083  $\mu$ M CTR-Hlp; lane 10, 0.166  $\mu$ M CTR-Hlp; lane 11, 0.33  $\mu$ M CTR-Hlp; lane 12, 0.083  $\mu$ M (CTR-Hlp + RL-Hlp); lane 13, 0.166  $\mu$ M (CTR-Hlp + RL-Hlp); lane 14, 0.33  $\mu$ M (CTR-Hlp + RL-Hlp). PT, primary transcript; RM, recovery marker. (B) Total RNA isolated from *M. smegmatis*. Lane 1, ssRNA marker; lane 2, total RNA from exponentially growing cells; lane 3, total RNA after 24 h of cold shock at 10  $^{\circ}$ C; lane 4, total RNA after 1 h recovery at 37  $^{\circ}$ C after cold shock.

The cold-shock response in *M. smegmatis* is poorly defined but involves the upregulation of several proteins, including an approximately 10-fold upregulation of Hlp (24). To investigate the *in vivo* effect of cold shock on transcription in *M. smegmatis*, total RNA was purified from exponentially growing cells and cold-shocked cells (Figure 10B). The amount of total RNA after 24 h of cold shock was compared to total RNA isolated from exponentially growing cells (Figure 10B, lanes 2 and 3) by measuring spot density of the main rRNA bands separately. After 24 h of cold shock, the large rRNA is reduced by 50% and the small rRNA by 70%, suggesting repression of transcription. While this observation does not address the role of Hlp in transcriptional regulation *in vivo*, it is consistent with the *in vitro* observation of transcriptional repression by Hlp. Cells allowed to recover after cold shock for 1 h at 37  $^{\circ}$ C did not show any significant increase in total RNA yield (Figure 10B, lane 4).

## DISCUSSION

*M. smegmatis* Hlp Has Two DNA Binding Domains. Mycobacterial Hlp differs from most other HU proteins by combining a proline-, alanine-, and lysine-repeat-rich C-terminal domain with the HU homologous domain. In *M. smegmatis* Hlp, both the N-terminal HU homologous domain (RL-Hlp) and the CTR domain contribute to the very high affinity for DNA (Figure 2), an affinity that is substantially higher than that of other HU proteins. The 76 bp DNA used for affinity measurements does not have propensity for adopting unusual structures, indicating that the high affinity

of Hlp is unrelated to topology of the DNA. Not only do both Hlp domains contribute to the nonspecific, high-affinity DNA binding, allowing Hlp to bind multiple DNA sites simultaneously, the CTR domain itself likely is multivalent. For histone H1, which was shown to be divalent, binding to linear DNA resulted in formation of protein–DNA aggregates unable to enter the gel matrix, a property also characteristic of Hlp. Binding of multiple DNAs by the isolated CTR domain is further demonstrated by its ability to enhance DNA end-joining.

To ascertain whether amino acids immediately following the HU-fold are essential, TL-Hlp was constructed. As seen from the considerably reduced DNA binding by TL-Hlp (Figure 4), the region intermediate to the N-terminal domain and the CTR is indeed required for DNA binding. Similarly, DNA binding was lost on removal of carboxy-terminal extensions from *E. coli* integration host factor (IHF) and the *Bacillus subtilis* phage SPO1-encoded TF1 to generate  $\sim$ 90 amino acid variants (30–34). Truncation of the last 10 amino acids of the IHF subunit HimD, which removed the C-terminal  $\alpha$ -helix, caused a 50–100-fold reduction in binding affinity, leading to the proposal that the C-terminal  $\alpha$ -helix plays an important role in stabilizing the complex. On the other hand, removal of the C-terminal  $\alpha$ -helix from the other subunit, HimA, caused IHF to lose binding specificity as this C-terminal helix is thought to be associated with stabilization of the arm structure by interacting with the turn between  $\alpha$ 3-helix and  $\beta$ 1; very weak and nonspecific binding was seen after removal of nine C-terminal amino acids (32). As for TF1 and IHF, it is possible that residues immediately C-terminal to the HU-fold of Hlp adopt an  $\alpha$ -helical structure that contributes to stability and function of the intercalating  $\beta$ -arms.

Roles in homologous DNA recombination have been shown or inferred based on preferred binding of HU proteins to four-way junctions (10). However, while *E. coli* HU binds the junction crossover, DrHU was shown to bind symmetrically to a pair of junction arms away from the point of crossover (15). DrHU features a 47-residue N-terminal extension carrying three lysine-rich repeats akin to those of the Hlp C-terminal domain. Given the larger size of Hlp, it may likewise bind at a distance from the junction crossover. For the 118-residue RL-Hlp, the affinity for four-way junction DNA is also not enhanced, but discrete complexes may be discerned (Figure 5); for RL-Hlp we surmise that topological constraints imposed by the junction structure may abrogate the significant cooperativity seen with linear duplex DNA. In the absence of the repeats, the observed cooperative DNA binding could result from protein–protein interaction, enabled by exposing residues that are otherwise buried in the full-length protein. Alternatively, global changes of DNA conformation upon initial complex formation may energetically favor additional protein binding (36). We also surmise that the failure of RL-Hlp to mediate intramolecular DNA cyclization reflects not a lack of DNA bending but accretion of additional protein molecules, resulting in out-of-phase bending and overall stiffening of the DNA. The inability of the full-length Hlp to cyclize DNA in the presence of T4 DNA ligase may result from interactions with the CTR that “stiffen” the DNA. This interpretation is supported by the observation that Hlp prevents intramolecular cyclization of 315 bp DNA (Figure 9).

Histone H1 has been shown to unwind DNA, to form doughnut-shaped complexes with double stranded DNA and to be involved in DNA condensation (37). Though CTR and histone H1 share an abundance of lysine-rich repeats, they exhibit different modes of DNA interaction; histone H1 binds preferentially to supercoiled DNA over relaxed or linear DNA while CTR exhibits no such preference (29). Evidently, Hlp binds DNA with high affinity, and both domains participate in DNA binding. No evidence of DNA bending by Hlp is observed; while the HU related domain would be predicted to engage DNA as seen for other homologues, interaction with the CTR may "stiffen" the DNA, thus preventing intramolecular ring closure (Figures 6 and 9).

*Hlp Promotes DNA End-Joining.* *M. smegmatis* is an obligate aerobe that resides in soil and has an unusually thick cell wall to prevent desiccation, yet extreme environmental conditions can cause serious desiccation and double-strand breaks in the chromosomal DNA (38, 39). Nonhomologous end-joining (NHEJ) has evolved in mycobacteria as a predominant repair mechanism for DNA double-strand breaks, in which short homologous DNA sequences called microhomologies serve as a protection mechanism against dehydration-related DNA damage (40–43). When in a dormant state with no active DNA replication, NHEJ has been predicted to be an active DNA repair mechanism (44, 45). The NHEJ apparatus in mycobacteria is constituted with mycobacterial Ku protein and ligase D (46, 47). Mycobacteria also encode five functional DNA ligases (41), more than other bacterial species, suggesting a higher occurrence of DNA ligation. Under anoxia or cold shock-induced dormancy, several proteins are upregulated, including Hlp (24). Though subject to further investigation, the unique CTR-mediated ability of Hlp to enhance DNA end-joining in the presence of T4 DNA ligase *in vitro* (Figure 6), along with its ability to bind more than one DNA molecule (Figure 3B), could place Hlp as a potential candidate in NHEJ-mediated DNA repair pathways, probably acting in conjunction with one of the many functional ligases encoded by mycobacteria. NHEJ-mediated DNA repair is not present in *E. coli*, but *M. tuberculosis* Ku protein and Ligase D can replace RecA and RecB mediated repair pathways in *E. coli* (40). HU proteins are abundant *in vivo*, yet regulated based on cell growth; *M. smegmatis* Hlp is upregulated under stressful conditions that demand unique responses, consistent with a function distinct from that of other HU homologues.

*Hlp Acts as a Transcriptional Repressor In Vitro.* *M. tuberculosis* and *M. smegmatis* both can sustain a long period of dormancy under unfavorable conditions and resume growth when favorable conditions return. During the onset of dormancy, due to cold shock or anoxia, both species show a considerable reduction or complete shutdown of protein synthesis (24, 48). Very little is known about the molecular processes *in vivo* pertaining to the onset of dormancy. With a considerable amount of debate, there are two existing models, one suggesting that formation of dormant or nonculturable cells is an adaptive measure genetically programmed to create viable but nonculturable cells, while the other theory proposes stochastic deterioration (49–51). Generally, bacterial responses to cold shock are mediated through adjustments in cell membrane fluidity and stabilization of DNA and RNA secondary structures, which may in turn decrease the efficiency of transcription, translation, and

DNA replication (52). In *E. coli*, cold-inducible proteins, such as CspA (for which a putative homologue is also found in mycobacteria), act as RNA chaperones to destabilize the RNA secondary structure, allowing cells to overcome the deleterious effects of cold shock on transcription and translation (52). Not much is known about the involvement of nucleoid-associated proteins in response to cold shock. H-NS in *E. coli* has been shown to be important for survival in response to cold shock and is thought to mediate transcriptional repression of the osmotic shock genes (53, 54). Sequencing of the *M. tuberculosis* genome revealed the presence of a putative H-NS homologue, but not much is known about its physiological function. Whether Hlp contributes to transcriptional repression *in vivo* in response to cold shock has yet to be determined, but indirect observations such as reduced metabolic adaptability of Hlp deletion mutants and downregulation of Hlp after 24 h of cold shock, as well as *in vitro* transcriptional repression, would be consistent with such activity.

Whether Hlp is involved in repression of transcription at specific promoters is unknown, but its high affinity and low cellular abundance suggest that it may be actively recruited to specific promoters. For example, active recruitment of mycobacterial H-NS-like protein Lsr2 to certain promoters has been shown to regulate transcription in both *M. tuberculosis* and *M. smegmatis*; like Hlp, Lsr2 is capable of intramolecular bridging of DNA, resulting in transcriptional repression (55, 56). The transcriptional repression is only achieved by full-length Hlp (Figure 10A, lanes 3–5) and is evidently not merely due to DNA occlusion by high-affinity binding, as the poly-lysine-like CTR alone does not repress transcription. The inability of RL-Hlp to repress transcription is consistent with the observation that *E. coli* HU does not obstruct but rather stimulates activity of T7 RNA polymerase (35). When both RL-Hlp and CTR are present in the reaction as separate polypeptides, no repression is seen, perhaps because cooperative binding by RL-Hlp excludes CTR binding to DNA. Cooperative binding appears to be abolished in full-length protein, likely resulting in a binding mode in which the HU domain and the CTR alternately engage the DNA. Such binding mode may promote a repressive intramolecular DNA bridging such as that suggested for Lsr2 (56). Hlp may either prevent recruitment of T7 RNA polymerase or interfere with elongation, in contrast to *E. coli* HU which enhances transcription by changing DNA superhelicity and stabilizing open complexes (35). While the effect of Hlp on the multisubunit bacterial RNA polymerase may differ from its effect on T7 RNA polymerase activity, the observation that Hlp and *E. coli* HU have opposite effects on the enzyme speaks to differential modes of DNA binding; considering the multivalent nature of Hlp, it is possible that extensive DNA looping may mimic a knotted DNA topology, previously shown to attenuate transcriptional activity by T7 RNA polymerase (57).

Homologues of other nucleoid-associated proteins, including H-NS, IHF, and Dps, have been identified in mycobacteria. However, little is known about nucleoid structure in this eubacterial family, and added complexity derives from the lack of conservation or distribution among the mycobacteria; for instance, mycobacterial IHF is unrelated to the HU protein family, and no Dps homologue is encoded in *M. tuberculosis*. Notably, the ability of mycobacterial Lsr2



to bridge distant DNA sites suggests its potential role in nucleoid organization. Considering the low cellular abundance and upregulation under stress, we propose that Hlp serves primary functions that may involve DNA double-strand break repair by enhancing end-joining and regulation of gene activity as opposed to global nucleoid organization.

## REFERENCES

- Rouvière-Yaniv, J. (1978) Localization of the HU protein on the *Escherichia coli* nucleoid. *Cold Spring Harbor Symp. Quant. Biol.* 42, 439–447.
- Boubrik, F., and Rouvière-Yaniv, J. (1995) Increased sensitivity to gamma irradiation in bacteria lacking protein HU. *Proc. Natl. Acad. Sci. U.S.A.* 92, 3958–3962.
- Dixon, N. E., and Kornberg, A. (1984) Protein HU in the enzymatic replication of the chromosomal origin of *Escherichia coli*. *Proc. Natl. Acad. Sci. U.S.A.* 81, 424–428.
- Craigie, R., Arndt-Jovin, D. J., and Mizuuchi, K. (1985) A defined system for the DNA strand-transfer reaction at the initiation of bacteriophage Mu transposition: protein and DNA substrate requirements. *Proc. Natl. Acad. Sci. U.S.A.* 82, 7570–7574.
- Guo, F., and Adhya, S. (2007) Spiral structure of *Escherichia coli* HUalpha-beta provides foundation for DNA supercoiling. *Proc. Natl. Acad. Sci. U.S.A.* 104, 4309–4314.
- Rice, P. A., Yang, S., Mizuuchi, K., and Nash, H. A. (1996) Crystal structure of an IHF-DNA complex: a protein-induced DNA U-turn. *Cell* 87, 1295–1306.
- Mouw, K. W., and Rice, P. A. (2007) Shaping the *Borrelia burgdorferi* genome: crystal structure and binding properties of the DNA-binding protein Hbb. *Mol. Microbiol.* 63, 1319–1330.
- Vis, H., Mariani, M., Vorgias, C. E., Wilson, K. S., Kaptein, R., and Boelens, R. (1995) Solution structure of the HU protein from *Bacillus stearothermophilus*. *J. Mol. Biol.* 254, 692–703.
- Swinger, K. K., Lemberg, K. M., Zhang, Y., and Rice, P. A. (2003) Flexible DNA bending in HU-DNA cocrystal structures. *EMBO J.* 22, 3749–3760.
- Kamashev, D., and Rouvière-Yaniv, J. (2000) The histone-like protein HU binds specifically to DNA recombination and repair intermediates. *EMBO J.* 19, 6527–6535.
- Balandina, A., Kamashev, D., and Rouvière-Yaniv, J. (2002) The bacterial histone-like protein HU specifically recognizes similar structures in all nucleic acids. DNA, RNA, and their hybrids. *J. Biol. Chem.* 277, 27622–27628.
- Castaing, B., Zelwer, C., Laval, J., and Boiteux, S. (1995) HU protein of *Escherichia coli* binds specifically to DNA that contains single-strand breaks or gaps. *J. Biol. Chem.* 270, 10291–10296.
- Grove, A., and Lim, L. (2001) High-affinity DNA binding of HU protein from the hyperthermophile *Thermotoga maritima*. *J. Mol. Biol.* 311, 491–502.
- Kamau, E., Tsihlis, N. D., Simmons, L. A., and Grove, A. (2005) Surface salt bridges modulate the DNA site size of bacterial histone-like HU proteins. *Biochem. J.* 390, 49–55.
- Ghosh, S., and Grove, A. (2004) Histone-like protein HU from *Deinococcus radiodurans* binds preferentially to four-way DNA junctions. *J. Mol. Biol.* 337, 561–571.
- Chen, C., Ghosh, S., and Grove, A. (2004) Substrate specificity of *Helicobacter pylori* histone-like HU protein is determined by insufficient stabilization of DNA flexure points. *Biochem. J.* 383, 343–351.
- Lewis, D. E., Geanakopoulos, M., and Adhya, S. (1999) Role of HU and DNA supercoiling in transcription repression: specialized nucleoprotein repression complex at gal promoters in *Escherichia coli*. *Mol. Microbiol.* 31, 451–461.
- Hwang, D. S., and Kornberg, A. (1992) Opening of the replication origin of *Escherichia coli* by DnaA protein with protein HU or IHF. *J. Biol. Chem.* 267, 23083–23086.
- Broyles, S. S., and Pettijohn, D. E. (1986) Interaction of the *Escherichia coli* HU protein with DNA. Evidence for formation of nucleosome-like structures with altered DNA helical pitch. *J. Mol. Biol.* 187, 47–60.
- Alonso, J. C., Gutierrez, C., and Rojo, F. (1995) The role of chromatin-associated protein Hbsu in beta-mediated DNA recombination is to facilitate the joining of distant recombination sites. *Mol. Microbiol.* 18, 471–478.
- Köhler, P., and Marahiel, M. A. (1997) Association of the histone-like protein HBSu with the nucleoid of *Bacillus subtilis*. *J. Bacteriol.* 179, 2060–2064.
- Mukherjee, A., Sokunbi, A. O., and Grove, A. (2008) DNA compaction by histone-like protein HU from the hyperthermophilic eubacterium *Thermotoga maritima*. *Nucleic Acids Res.* 36, 3956–3968.
- Prabhakar, S., Annapurna, P. S., Jain, N. K., Dey, A. B., Tyagi, J. S., and Prasad, H. K. (1998) Identification of an immunogenic histone-like protein (HLPmt) of *Mycobacterium tuberculosis*. *Tuber. Lung Dis.* 79, 43–53.
- Shires, K., and Steyn, L. (2001) The cold-shock stress response in *Mycobacterium smegmatis* induces the expression of a histone-like protein. *Mol. Microbiol.* 39, 994–1009.
- Lee, B. H., Murugasu-Oei, B., and Dick, T. (1998) Upregulation of a histone-like protein in dormant *Mycobacterium smegmatis*. *Mol. Gen. Genet.* 260, 475–479.
- Pethe, K., Puech, V., Daffe, M., Josenhans, C., Drobecq, H., Loch, C., and Menozzi, F. D. (2001) *Mycobacterium smegmatis* laminin-binding glycoprotein shares epitopes with *Mycobacterium tuberculosis* heparin-binding haemagglutinin. *Mol. Microbiol.* 39, 89–99.
- Krasilnikova, M. M., Samadashwily, G. M., Krasilnikov, A. S., and Mirkin, S. M. (1998) Transcription through a simple DNA repeat blocks replication elongation. *EMBO J.* 17, 5095–5102.
- Tsihlis, N. D., and Grove, A. (2006) The *Saccharomyces cerevisiae* RNA polymerase III recruitment factor subunits Brf1 and Bdp1 impose a strict sequence preference for the downstream half of the TATA box. *Nucleic Acids Res.* 34, 5585–5593.
- Ellen, T. P., and van Holde, K. E. (2004) Linker histone interaction shows divergent character with both supercoiled and linear DNA. *Biochemistry* 43, 7867–7872.
- Granston, A. E., and Nash, H. A. (1993) Characterization of a set of integration host factor mutants deficient for DNA binding. *J. Mol. Biol.* 234, 45–59.
- Mengeritsky, G., Goldenberg, D., Mendelson, I., Giladi, H., and Oppenheim, A. B. (1993) Genetic and biochemical analysis of the integration host factor of *Escherichia coli*. *J. Mol. Biol.* 231, 646–657.
- Sayre, M. H., and Geiduschek, E. P. (1988) TF1, the bacteriophage SPO1-encoded type II DNA-binding protein, is essential for viral multiplication. *J. Virol.* 62, 3455–3462.
- Andera, L., and Geiduschek, E. P. (1994) Determinants of affinity and mode of DNA binding at the carboxy terminus of the bacteriophage SPO1-encoded type II DNA-binding protein, TF1. *J. Bacteriol.* 176, 1364–1373.
- Zulianello, L., van Ulsen, P., van de Putte, P., and Goosen, N. (1995) Participation of the flank regions of the integration host factor protein in the specificity and stability of DNA binding. *J. Biol. Chem.* 270, 17902–17907.
- Morales, P., Rouvière-Yaniv, J., and Dreyfus, M. (2002) The histone-like protein HU does not obstruct movement of T7 RNA polymerase in *Escherichia coli* cells but stimulates its activity. *J. Bacteriol.* 184, 1565–1570.
- Rudnick, J., and Bruinsma, R. (1999) DNA-protein cooperative binding through variable-range elastic coupling. *Biophys. J.* 76, 1725–1733.
- Hsiang, M. W., and Cole, R. D. (1977) Structure of histone H1-DNA complex: effect of histone H1 on DNA condensation. *Proc. Natl. Acad. Sci. U.S.A.* 74, 4852–4856.
- Potts, M. (1994) Desiccation tolerance of prokaryotes. *Microbiol. Rev.* 58, 755–805.
- Dose, K., Bieger-Dose, A., Kerz, O., and Gill, M. (1991) DNA-strand breaks limit survival in extreme dryness. *Orig. Life Evol. Biosph.* 21, 177–187.
- Malyarchuk, S., Wright, D., Castore, R., Klepper, E., Weiss, B., Doherty, A. J., and Harrison, L. (2007) Expression of *Mycobacterium tuberculosis* Ku and Ligase D in *Escherichia coli* results in RecA and RecB-independent DNA end-joining at regions of microhomology. *DNA Repair* 6, 1413–1424.
- Gong, C., Bongiorno, P., Martins, A., Stephanou, N. C., Zhu, H., Shuman, S., and Glickman, M. S. (2005) Mechanism of nonhomologous end-joining in mycobacteria: a low-fidelity repair system driven by Ku, ligase D and ligase C. *Nat. Struct. Mol. Biol.* 12, 304–312.
- Stephanou, N. C., Gao, F., Bongiorno, P., Ehrst, S., Schnappinger, D., Shuman, S., and Glickman, M. S. (2007) Mycobacterial nonhomologous end joining mediates mutagenic repair of chromosomal double-strand DNA breaks. *J. Bacteriol.* 189, 5237–5246.

43. Pitcher, R. S., Green, A. J., Brzostek, A., Korycka-Machala, M., Dziadek, J., and Doherty, A. J. (2007) NHEJ protects mycobacteria in stationary phase against the harmful effects of desiccation. *DNA Repair* 6, 1271–1276.
44. Weller, G. R., Kysela, B., Roy, R., Tonkin, L. M., Scanlan, E., Della, M., Devine, S. K., Day, J. P., Wilkinson, A., d'Adda di Fagagna, F., Devine, K. M., Bowater, R. P., Jeggo, P. A., Jackson, S. P., and Doherty, A. J. (2002) Identification of a DNA nonhomologous end-joining complex in bacteria. *Science* 297, 1686–1689.
45. Bowater, R., and Doherty, A. J. (2006) Making ends meet: repairing breaks in bacterial DNA by non-homologous end-joining. *PLoS Genet.* 2, e8.
46. Della, M., Palmbo, P. L., Tseng, H. M., Tonkin, L. M., Daley, J. M., Topper, L. M., Pitcher, R. S., Tomkinson, A. E., Wilson, T. E., and Doherty, A. J. (2004) Mycobacterial Ku and ligase proteins constitute a two-component NHEJ repair machine. *Science* 306, 683–685.
47. Pitcher, R. S., Tonkin, L. M., Green, A. J., and Doherty, A. J. (2005) Domain structure of a NHEJ DNA repair ligase from *Mycobacterium tuberculosis*. *J. Mol. Biol.* 351, 531–544.
48. Hu, Y. M., Butcher, P. D., Sole, K., Mitchison, D. A., and Coates, A. R. (1998) Protein synthesis is shutdown in dormant *Mycobacterium tuberculosis* and is reversed by oxygen or heat shock. *FEMS Microbiol. Lett.* 158, 139–145.
49. Nystrom, T. (2001) Not quite dead enough: on bacterial life, culturability, senescence, and death. *Arch. Microbiol.* 176, 159–164.
50. Barer, M. R., and Harwood, C. R. (1999) Bacterial viability and culturability. *Adv. Microb. Physiol.* 41, 93–137.
51. Mukamolova, G. V., Kaprelyants, A. S., Kell, D. B., and Young, M. (2003) Adoption of the transiently non-culturable state—a bacterial survival strategy. *Adv. Microb. Physiol.* 47, 65–129.
52. Padhtare, S., Yamanaka, K., and Inouye, M. (2000) The cold shock response, in *The Bacterial Stress Responses* (Storz, G., and Hengge-Aronis, R., Eds.) pp 33–45, ASM Press, Washington, DC.
53. Dersch, P., Kneip, S., and Bremer, E. (1994) The nucleoid-associated DNA-binding protein H-NS is required for the efficient adaptation of *Escherichia coli* K-12 to a cold environment. *Mol. Gen. Genet.* 245, 255–259.
54. Stella, S., Falconi, M., Lammi, M., Gualerzi, C. O., and Pon, C. L. (2006) Environmental control of the *in vivo* oligomerization of nucleoid protein H-NS. *J. Mol. Biol.* 355, 169–174.
55. Colangeli, R., Helb, D., Vilchèze, C., Hazbón, M. H., Lee, C. G., Safi, H., Sayers, B., Sardone, I., Jones, M. B., Fleischmann, R. D., Peterson, S. N., Jacobs, W. R., Jr., and Alland, D. (2007) Transcriptional regulation of multi-drug tolerance and antibiotic-induced responses by the histone-like protein Lsr2 in *M. tuberculosis*. *PLoS Pathog.* 3, e87.
56. Chen, J. M., Ren, H., Shaw, J. E., Wang, Y. J., Li, M., Leung, A. S., Tran, V., Berbenetz, N. M., Kocíncová, D., Yip, C. M., Reyrat, J. M., and Liu, J. (2008) Lsr2 of *Mycobacterium tuberculosis* is a DNA-bridging protein. *Nucleic Acids Res.* 36, 2123–2135.
57. Portugal, J., and Rodriguez-Campos, A. (1996) T7 RNA polymerase cannot transcribe though a highly knotted DNA template. *Nucleic Acids Res.* 24, 4890–4894.

BI800010S